Vital Annex: International Journal of Novel Research in Advanced Sciences
ISSN: 2751-756X
Volume 04 Number 05 (2025)
https://innosci.org/IJNRAS

Article

Solvent Effects on Structural and Electronic Properties of Lomustine Combined With DFT Method

Abdul Hakim Sh. Mohammed[1]

1. Department of Physics, College of Education, University of Kirkuk, Kirkuk, Iraq
* Correspondence: hakimsh@uokirkuk.edu.iq

Abstract: The objective of this work is to examine the solute-solvent interactions by using optimised conformations of lomustine in various solvents and UV-Vis spectra by DFT calculations. The adjusted geometry of lomustine in the gas phase and in chloroform, acetone, ethanol, and water was estimated. A theoretical investigation of the potential stable formation of lomustine was conducted in various solvents using DFT/B3LYP with the 6-311G+(d) basis set. The findings indicate that the structural bonds vary with the solvent's polarity and solvation energy. The effects of solvents on lomustine were investigated using the conductor-like polarisable continuum model (CPCM) technique. The electronic absorption spectra of the molecule was assessed using the time-dependent density functional theory (TD/DFT) approach at the same level of analysis. In this work, the energy gap (HOMO–LUMO) was determined by quantum chemical calculations. The Frontier Molecular Orbital (FMO) investigation examined the highest occupied molecular orbital (HOMO) values of the molecule in several solvents, yielding -7.2530 eV for chloroform, -7.2533 eV for acetone, -7.2533 eV for ethanol, and -7.2533 eV for water. Their lowest unoccupied molecular orbital (LUMO) values were -2.4947 eV, -2.4882 eV, -2.4877 eV, and -2.4866 eV, resulting in corresponding band gaps of 4.7583 eV, 4.7651 eV, 4.7656 eV, and 4.7667 eV. Notably, water solvent had the largest energy gap (4.7667 eV) among the solvents used, indicating elevated kinetic energy and substantial chemical reactivity.

Keywords: lomustine, solvents, UV-Vis spectra, frontier HOMO-LUMO, DFT

Citation: Mohammed A. H. Sh. Solvent Effects on Structural and Electronic Properties of Lomustine Combined With DFT Method. Vital Annex: International Journal of Novel Research in Advanced Sciences 2025, 4(5), 158-166.

Received: 04th Mar 2025
Revised: 11th Apr 2025
Accepted: 24th May 2025
Published: 10th Jun 2025

1. Introduction

One-(2-Chloroethyl)-3-cyclohexyl-1-nitrosourea is the chemical formula of lomustine. It is N-nitrosourea, which is a urea in which one of the nitrogen atoms is replaced by a cyclohexyl group and the other by a 2-chloroethyl group and a nitroso group [1]. It has a role as an alkylating and an antineoplastic agent [2, 3] , it is used in the treatment of brain tumors [4], lung cancer [5, 6], malignant melanoma and other solid tumors. It is a member of N-nitrosoureas and an organ chlorine compound [7].

The impact of solvents is crucial for future pharmaceutical research and formulation, since they modify the medicine by facilitating its release inside the body. Structural geometry and electronic absorption spectra are often used to investigate solute-solvent interactions and serve as very accurate instruments. Furthermore, alterations in the absorption bands of molecules in various solvents (bathochromic or hypochromic shifts) are referred to as solvatochromism and are contingent upon the electronic structure of both the molecule and the solvent. This study aims to analyse the structural properties and UV-Vis spectrum of lomustine using theoretical methods (DFT calculations) due to the absence of literature on solvent effects regarding this compound. The DFT-B3LYP method is

considered one of the most commonly used computational methods in compounds studies because its results agree well with experimental results [8, 9].

2. Materials and Methods

Every calculation were conducted with the Gaussian 09 W software package and Gauss View 5.0.9 for presentation [10,11]. The optimised geometry of lomustine was computed using DFT/B3LYP with the 6-311+G(d) basis set [12]. Compared calculation were conducted for chloroform, acetone, ethanol, and aqueous solutions of lomustine. All calculations concerning solvent effects used the conductor-like polarisation continuum model (CPCM) [13]. To examine the energetic behaviour of molecules in solvent media, the conductor-like polarisation continuum model (CPCM) was used, and the initial process was repeated using chloroform, acetone, ethanol, and water. The electronic absorption spectra were calculated using time-dependent density functional theory (TD/DFT) [14, 15], including solvent effects (chloroform, acetone, ethanol, water).

Utilising the same functional and basis set, we acquired excited states that permit a minimum of three singlet-to-singlet spin transitions. The HOMO-LUMO gap values were used to determine the frontier orbitals, which then facilitated the calculation of global hardness (η), global softness (S), electronegativity (χ), chemical potential (μ), and electrophilicity index (ω) descriptors.

3. Results and Discussion

Molecular geometries

The molecular geometry and atom numbering used in this study is shown in Figure 1. First, the geometry was optimized for gas phase, then, re-optimized in the various media. The total energy, dipole moment and free solvation energies (ΔG) of lomustine in various media using DFT/B3LYP 6-311G+(d) are given in Table 1. The estimated results to point to that the lomustine dipole moment dissolved (in chloroform, acetone, ethanol and water) increased when the solvent polarity increased. The most important feature of the interaction between any solute and the solvent is best described using the solvation free energy [16]. Therefore, the free energy of solute-solvent interaction was calculated for the solutes of lomustine (in chloroform, acetone, ethanol, and water). The results showed that lomustine with a large dipole moment dissolved in water showed the most negative ΔG values. The calculations showed that the solvation free energy (ΔG) of lomustine is chloroform < acetone < ethanol < water, respectively.

The ideal bond lengths and angles for this chemical were computed in the gas phase and in chloroform, acetone, ethanol, and water, as shown in Table 2.When comparing bond lengths in the gas phase to those in solvents, the solvent effect results in variations in the predicted geometries of lomustine in solution. However, the values for acetone, ethanol, and water are almost identical due to the polar nature of these solvents.

The molecular structure of lomustine has four primary bond lengths: C-C, C=O, C-N, and N=O. Table 2 indicates that the aliphatic bond length between C17 and C20 is comparatively low relative to other C-C bonds within the cyclic ring. This is attributed to the fact that aliphatic bond lengths are typically shorter than cyclic bond lengths due to electronic effects (hybridisation), steric effects (ring strain, torsional strain), and geometric effects (bond angle). The remaining C-N bonds exhibit varying values contingent upon the substituents.The C3-N12 bond length exceeds that of other C14-N12 bonds because C14 and N12 are bonded to the carbonyl carbon (C14=O16), which also applies to the bonds (C17-N15) and (C14-N15). In all solvents, the bond lengths remain rather consistent throughout the media, however the bond lengths of N15-N30 in all solvents (0.0078, 0.0094, 0.0095, 0.0098 for chloroform, acetone, ethanol, and water, respectively) exhibit an increase in comparison to the gas phase as solvent polarity rises. This significant fluctuation is attributable to the electrostatic interaction between the solute and the solvent. In all solvents, the bond angles are fairly uniform with minor deviations. Conversely, the most

significant divergence of the C3-N12-H13, C3-N12-C14, and C17-C20-H22 angles, around 0.5°, is seen in the solvents relative to the gaseous state. This significant alteration is attributable to intramolecular hydrogen bonding and electrostatic interactions between the solute and the solvent.This image displays the optimized molecular geometry of a complex organic compound, likely derived from quantum chemical calculations (e.g., DFT). Color coding indicates atom types: carbon (gray), hydrogen (white), nitrogen (blue), oxygen (red), and chlorine (green). The structure reveals aromatic rings, functional groups (such as amides or carboxamides), and a halogen substituent—features relevant for pharmacological or electronic properties (Figure 1).

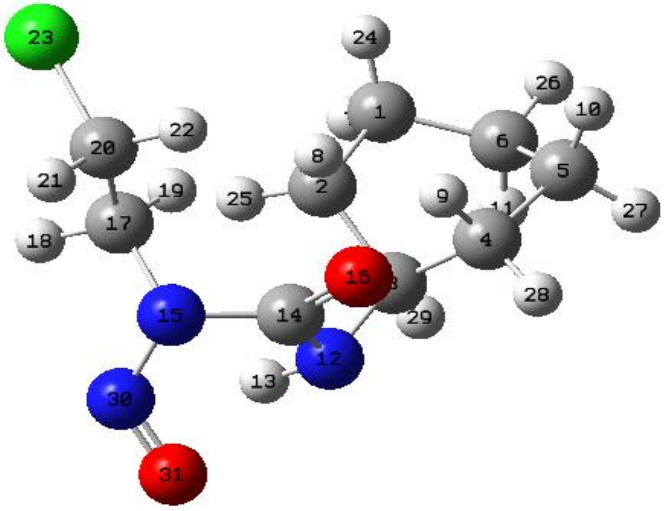

Figure 1. Lomustine structure

The table demonstrates solvent-dependent variations in energy, dipole moment, and Gibbs free energy (ΔG). As solvent polarity increases from vacuum to water, dipole moments rise and ΔG values become more negative, indicating enhanced stabilization in polar media, with water yielding the most favorable energetic and electronic stabilization for the studied molecule (Table 1).

Table 1: Calculated total energies (E), dipole moments, solvation-free energies (ΔG) (kJ/mol) of lomustine in different media.

Medium	E(Hartrees)	Dipole moments (Debye)	ΔG(kJ/mol)
Vacuum	-1127.6426	3.2084	
Chloroform	-1127.6497	3.7973	-18.77
Acetone	-1127.6515	3.9597	-23.31
Ethanol	-1127.6516	3.9688	-23.55
Water	-1127.6519	3.9983	-24.35

The tables present a comprehensive analysis of bond lengths and bond angles of the studied molecule in different solvent environments. Minor but consistent variations are observed across vacuum, chloroform, acetone, ethanol, and water. Increasing solvent polarity correlates with subtle decreases in bond lengths and nuanced shifts in bond angles, suggesting solvent-induced electronic reorganization and stabilization. These findings underscore the molecule's conformational sensitivity to its surrounding medium and highlight water as the environment inducing the most compact and polarized structure (Table 2).

Bond Lengths (A°)					
Bond	Vacuum	Chloroform	Acetone	Ethanol	Water
R(C1-C2)	1.543	1.5431	1.5431	1.5431	1.5431
R(C1-C6)	1.533	1.5332	1.5332	1.5332	1.5332
R(C1-H7)	1.0942	1.0942	1.0942	1.0942	1.0942
R(C1-H24)	1.096	1.096	1.0961	1.0961	1.0961

R(C2-C3)	1.55	1.5496	1.5496	1.5496	1.5496
R(C2-H8)	1.0912	1.0916	1.0917	1.0917	1.0917
R(C2-H25)	1.0953	1.0949	1.0947	1.0947	1.0947
R(C3-C4)	1.5355	1.5351	1.535	1.535	1.535
R(C3-N12)	1.4743	1.4755	1.4759	1.4759	1.4759
R(C3-H29)	1.0945	1.0934	1.0931	1.093	1.093
R(C4-C5)	1.5452	1.5453	1.5453	1.5453	1.5453
R(C4-H9)	1.0919	1.0921	1.0922	1.0922	1.0922
R(C4-H28)	1.0941	1.0939	1.0938	1.0938	1.0938
R(C5-C6)	1.549	1.549	1.549	1.549	1.549
R(C5-H10)	1.0944	1.0944	1.0944	1.0944	1.0944
R(C5-H27)	1.0953	1.095	1.0949	1.0949	1.0949
R(C6-H11)	1.0971	1.0968	1.0967	1.0967	1.0967
R(C6-H26)	1.094	1.0941	1.0941	1.0941	1.0941
R(N12-H13)	1.0121	1.0119	1.0119	1.0119	1.0119
R(N12-H14)	1.3433	1.339	1.3378	1.3378	1.3376
R(H14-N15)	1.4689	1.4717	1.4723	1.4723	1.4724
R(H14-O16)	1.2164	1.2193	1.2201	1.2202	1.2203
R(N15-C17)	1.4725	1.4733	1.4734	1.4734	1.4734
R(N15-N30)	1.3504	1.3426	1.341	1.3409	1.3406
R(C17-H18)	1.0886	1.0882	1.088	1.088	1.088
R(C17-H19)	1.0877	1.0872	1.087	1.087	1.087
R(C17-C20)	1.5252	1.525	1.525	1.525	1.525
R(C20-H21)	1.0889	1.0879	1.0876	1.0876	1.0876
R(C20-H22)	1.0867	1.0862	1.0861	1.0861	1.0861
R(C20-Cl23)	1.8118	1.818	1.8196	1.8196	1.8199
R(N30-O31)	1.2196	1.2235	1.2244	1.2244	1.2245
R(H13-O31)	1.8709	1.8729	1.8737	1.8737	1.8737
Angles (°)					
Angle	gas	Chloroform	Acetone	Ethanol	Water
A(2, 1, 6)	111.411	111.371	111.360	111.360	111.357
A(2, 1, 7)	109.691	109.643	109.630	109.630	109.627
A(2, 1, 24)	109.645	109.747	109.775	109.776	109.781
A(C6, C1, H7)	110.695	110.686	110.681	110.681	110.680
A(C6, C1, H24)	109.198	109.139	109.126	109.125	109.123
A(H7, C1, H24)	106.052	106.116	106.131	106.131	106.134
A(C1, C2, C3)	112.060	111.980	111.961	111.960	111.957
A(C1, C2, H8)	109.488	109.577	109.602	109.603	109.607
A(C1, C2, H25)	110.282	110.242	110.230	110.230	110.227
A(C3, C2, H8)	109.371	109.540	109.583	109.586	109.593
A(C3, C2, H25)	108.614	108.535	108.514	108.512	108.509
A(H8, C2, H25)	106.882	106.826	106.811	106.81	106.807
A(C2, C3, C4)	111.478	111.577	111.611	111.613	111.619
A(C2, C3, N12)	112.236	112.242	112.244	112.244	112.244
A(C2, C3, H29)	108.466	108.424	108.41	108.41	108.406
A(C4, C3, N12)	113.388	113.476	113.485	113.486	113.487
A(C4, C3, H29)	107.278	107.239	107.227	107.227	107.225
A(N12, C3, H29)	103.443	103.304	103.277	103.275	103.271

A(C3, C4, C5)	110.348	110.208	110.179	110.178	110.173
A(C3, C4, H9)	108.993	109.248	109.308	109.311	109.322
A(C3, C4, H28)	109.794	109.792	109.784	109.783	109.782
A(C5, C4, H9)	110.656	110.484	110.446	110.444	110.438
A(C5, C4, H28)	110.299	110.290	110.287	110.287	110.287
A(H9, C4, H28)	106.675	106.753	106.773	106.774	106.777
A(C4, C5, C6)	112.709	112.714	112.717	112.717	112.718
A(C4, C5, H10)	108.618	108.600	108.600	108.598	108.560
A(C4, C5, H27)	109.870	109.749	109.714	109.713	109.706
A(C6, C5, H10)	109.946	109.943	109.947	109.948	109.948
A(C6, C5, H27)	109.476	109.454	109.447	109.447	109.445
A(H10, C5, H27)	106.00	106.168	106.207	106.209	106.215
A(C1, C6, C5)	111.250	111.281	111.292	111.292	111.294
A(C1, C6, H11)	108.908	108.861	108.847	108.847	108.844
A(C1, C6, H26)	110.618	110.556	110.541	110.540	110.538
A(C5, C6, H11)	110.025	109.980	109.967	109.967	109.964
A(C5, C6, H26)	110.108	110.082	110.077	110.077	110.076
A(H11, C6, H26)	105.782	105.934	105.971	105.973	105.979
A(C3, N12, H13)	119.641	119.085	118.945	118.938	118.913
A(C3, N12, H14)	123.553	124.023	124.138	124.145	124.165
A(H13, N12, H14)	116.784	116.882	116.906	116.908	116.912
A(N12, H14, N15)	115.969	116.094	116.131	116.133	116.139
A(N12, H14, O16)	126.805	126.968	127.000	127.005	127.011
A(N15, H14, O16)	117.225	116.938	116.866	116.862	116.849
A(H14, N15, C17)	116.777	116.861	116.879	116.880	116.883
A(H14, N15, N30)	130.239	130.184	130.174	130.174	130.172
A(C17, N15, N30)	112.983	112.955	112.947	112.947	112.945
A(N15, C17, H18)	106.500	106.593	106.612	106.613	106.617
A(N15, C17, H19)	108.551	108.438	108.414	108.412	108.409
A(N15, C17, C20)	111.379	111.065	110.995	110.991	110.979
A(H18, C17, H19)	109.381	109.210	109.164	109.162	109.153
A(H18, C17, C20)	110.501	110.631	110.663	110.665	110.670
A(H19, C17, C20)	110.423	110.782	110.866	110.871	110.886

A(C17, C20, H21)	111.405	111.694	111.769	111.773	111.787
A(C17, C20, H22)	111.568	111.970	112.067	112.073	112.090
A(C17, C20, H23)	109.567	109.414	109.371	109.368	109.361
A(H21, C20, H22)	110.295	110.231	110.214	110.213	110.210
A(C21, C20, H23)	106.840	106.621	106.569	106.566	106.557
A(H22, C20, H23)	106.953	106.640	106.563	106.560	106.546
A(N15, N30, O31)	117.954	118.164	118.211	118.213	118.221

Table 2: Interatomic bond distances (A°) and bond angles (o) for the lomustine molecule in gas phase and different media.

UV-Vis Spectra analysis

The electronic transitions of the lomustine molecule were computed using time-dependent density functional theory (TD/DFT) and assessed using UV-Vis spectroscopy. Theoretical absorption spectra were obtained using chloroform, acetone, ethanol, and water as solvents. Figure 2 illustrates the theoretical absorption spectra of the title chemical in both the gas phase and the solvents used in this work. Table 3 encapsulates the computed wavelengths (λ), oscillator strengths (f), and electronic transitions corresponding to the peak absorption. The Gauss View 5.2 software was used to examine molecular orbitals and electronic transitions. Theoretical findings were used to elucidate the experimental absorption bands. Three peak absorbance bands were detected in the UV-Vis spectra of lomustine. The first two bands in the ethanol were identified at 228 nm and 278 nm, designated as a $\pi \rightarrow \pi^*$ transition. The computed values of the first two bands were 261.02 nm and 289.6 nm, respectively. The transition from HOMO-2 to LUMO occurs with a chance of 76%, whereas the transfer from HOMO-1 to LUMO occurs with a probability of 99%. A third band was identified in the ethanol spectra at 397 nm, with the theoretical value of 403.39 nm designated as the $n \rightarrow \pi^*$ transition. Theoretically, the computed values of the first two bands across all solvents exhibited red changes from chloroform to water, while the last band experienced a blue shift. The UV-Vis absorbance spectra reveal solvent-dependent shifts in peak intensity and position. The gas phase exhibits the lowest absorbance and a slight blue shift, while polar solvents like water and ethanol show red-shifted absorption maxima with increased intensity. This indicates enhanced solute-solvent interactions and stabilization of excited states in polar environments (Figure 2).

Figure 2: Maximum intensity on UV-Vis absorption spectra of lomustine in gas phase and dissolved in (chloroform, acetone, ethanol, and water

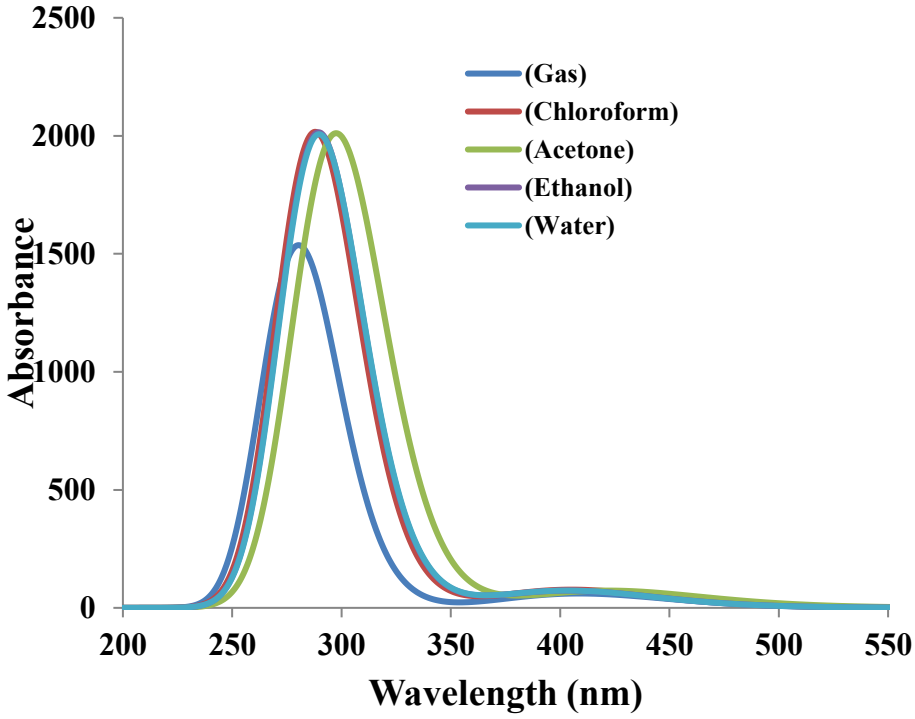

The table summarizes the solvent effects on electronic transitions. Across all media, the primary transition is HOMO → LUMO, with high contributions (≥97%) and strong oscillator strengths in the 288–290 nm range. Solvent polarity slightly red-shifts the λ_max and introduces secondary transitions (e.g., HOMO → LUMO+1), indicating enhanced intramolecular charge transfer in polar environments such as water and ethanol (Table 3).

Medium	Wavelength (λ/nm)	Oscillator strength (f)	Electronic transitions
Vacuum	408.74	0.0015	$HOMO \rightarrow LUMO$ (98%)
	280.44	0.0378	$HOMO-1 \rightarrow LUMO$ (98%)
	259.92	0.0003	$HOMO-3 \rightarrow LUMO$ (68%)
Chloroform	405.38	0.0019	$HOMO \rightarrow LUMO$ (97%)
	288.10	0.0496	$HOMO-1 \rightarrow LUMO$ (99%)
	260.82	0.0007	$HOMO-2 \rightarrow LUMO$ (74%)
Acetone	403.99	0.0018	$HOMO \rightarrow LUMO$ (97%)
	289.51	0.0495	$HOMO-1 \rightarrow LUMO$ (99%)
	261.01	0.0006	$HOMO-2 \rightarrow LUMO$ (76%)
Ethanol	403.93 (397)*	0.0018	$HOMO \rightarrow LUMO$ (97%)
	289.60 (278)*	0.0496	$HOMO-1 \rightarrow LUMO$ (99%)
	261.02 (228)*	0.0006	$HOMO-2 \rightarrow LUMO$ (76%)
Water	403.65	0.0018	$HOMO \rightarrow LUMO$ (97%)
	289.81	0.0494	$HOMO-1 \rightarrow LUMO$ (99%)
	261.05	0.0006	$HOMO-2 \rightarrow LUMO$ (76%)

*Experimental [17]

Table 3: Theoretical wavelengths of maximum absorption, oscillator strength (*f*) and the electronic transitions and experimental wavelengths of maximum absorption (in ethanol)

Frontier HOMO-LUMO

The frontier HOMO (the highest occupied molecular orbital) and LUMO (the lowest unoccupied molecular orbital) are the most important orbitals for the reactivity and kinetic stability of the molecule. DFT quantum chemical distributors provide insight into the effectiveness of molecules in pharmaceutical formulations [18]. Therefore, we calculated the energy band gap, hardness (η), softness (S), chemical potential (μ), electronegativity

(χ), and electrophilicity index (ω) of the HOMO and LUMO orbitals of lomustine in different media using the 6-311G+(d) basis set. The results are shown in Table 4. The analysis of gap values shows that lomustine in aqueous solution has high chemical hardness and good stability. The HOMO-LUMO frontier orbital composition of lomustine calculated using DFT/6-311G+(d) is shown in Figure 3. The highest occupied molecular orbital (HOMO) and lowest unoccupied molecular orbital (LUMO) were performed to estimate the orbital energy level behavior of the title compound. The HOMO and LUMO of the title compound are α molecular orbital level (62) and α molecular orbital level (63), respectively The energy value of the HOMO (62) orbital is -7.2511 eV and that of the LUMO (63) orbital is -2.5214 eV. The HOMO-LUMO energy gap was evaluated to be -2.5214 eV using isolated gas phase calculation. The high HOMO-LUMO energy gap means high kinetic energy and high chemical reactivity.

The table presents quantum chemical descriptors across different solvents. As polarity increases from vacuum to water, slight stabilization of both EHoMO and ELUMO is observed, leading to a marginal increase in the energy gap . Hardness and electrophilicity increase, while softness decreases, suggesting improved molecular stability and reactivity in polar environments (Table 4).

	Vacuum	Chloroform	Acetone	Ethanol	Water
E_{HOMO} (eV)	-7.2511	-7.2530	-7.2533	-7.2533	-7.2533
E_{LUMO} (eV)	-2.5214	-2.4947	-2.4882	-2.4877	-2.4866
E_g (eV)	4.7297	4.7583	4.7651	4.7656	4.7667
Hardness (η) (eV)	2.3649	2.3792	2.3826	2.3828	2.3834
Softness (S) (eV)	0.4229	0.4203	0.4197	0.4196	0.4195
Electronegativity (χ) (eV)	4.8863	4.8739	4.8708	4.8705	4.8700
Chemical potential (μ) (eV)	-4.8863	-4.8739	-4.8708	-4.8705	-4.8700
Electrophilicity index (ω) (eV)	5.0480	5.9922	5.9787	5.9777	5.9754

Table 4: Comparison of quantum chemical descriptors of lomustine in various media.

The image displays the molecular orbital distribution and energy gap between the HOMO and LUMO. The HOMO is delocalized over the aromatic and electron-donating regions, while the LUMO localizes over electron-withdrawing areas, indicating intramolecular charge transfer. The calculated gap reflects moderate electronic stability and reactivity (Figure 3).

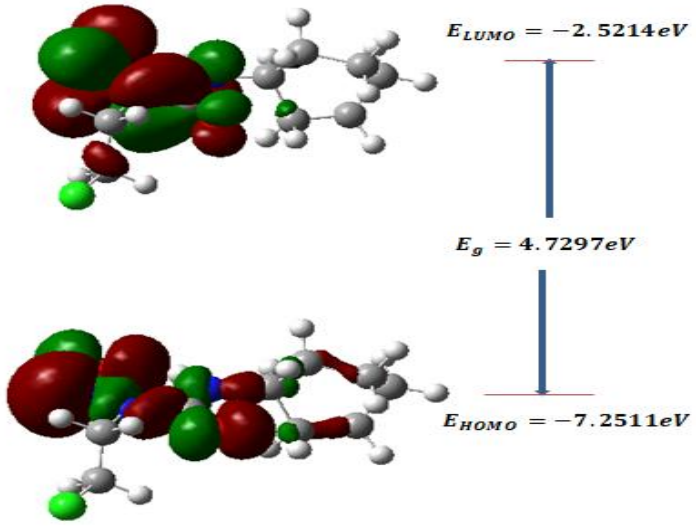

Figure 3. Frontier molecular diagram of lomustine in gas phase

4. Conclusion

In this study, structural characterization and UV-visible spectra were used for the first time to investigate the solvent effect of lomustine. The results showed that the dipole

moment of lomustine in solvents (chloroform, acetone, ethanol, and water) increases as the solvent polarity increases. Thus, as the solvent polarity increases, the molecular stability increases. Furthermore, lomustine with the largest dipole moment dissolved in water exhibited the most negative free solvation energy values. Geometric optimization calculations in four different solvents yielded the most stable structure of lomustine. The lowest energy state resulting from the optimization was also found in water. Furthermore, UV-Vis studies of lomustine showed that in polar solvents, a redshift appears in the absorption spectrum and the electronic dipole moment of the molecule increases in the absorbing phase. Finally, a slight red shift due to the solvent effect occurs in the absorption spectrum of lomustine.

REFERENCES

[1] S. Agarwal, D. K. Jangir, P. Singh, and R. Mehrotra, "Spectroscopic analysis of the interaction of lomustine with calf thymus DNA," J. Photochem. Photobiol. B: Biol., vol. 130, pp. 281–286, Jan. 2014.

[2] A. Mehrotra, R. C. Nagarwal, and J. K. Pandit, "Lomustine loaded chitosan nanoparticles: characterization and in vitro cytotoxicity on human lung cancer cell line L132," Chem. Pharm. Bull., vol. 59, no. 3, pp. 315–320, 2011.

[3] H. P. Lipp and J. T. Hartmann, "Cytostatic and cytotoxic drugs," in Side Effects of Drugs Annual, vol. 30, Elsevier, 2008, pp. 520–532.

[4] R. B. Weiss and B. F. Issell, "The nitrosoureas: carmustine (BCNU) and lomustine (CCNU)," Cancer Treat. Rev., vol. 9, pp. 313–330, 1982.

[5] B. Lebeau, C. Chouaïd, M. Baud, M. J. Masanès, and M. Febvre, "Oral second-and third-line lomustine–etoposide–cyclophosphamide chemotherapy for small cell lung cancer," Lung Cancer, vol. 67, no. 2, pp. 188–193, Feb. 2010.

[6] S. Bibi et al., "Investigation of the adsorption properties of gemcitabine anticancer drug with metal-doped boron nitride fullerenes as a drug-delivery carrier: a DFT study," RSC Adv., vol. 12, no. 5, pp. 2873–2887, 2022.

[7] C. T. Gnewuch and G. Sosnovsky, "Critical appraisals of approaches for predictive designs in anticancer drugs," Cell. Mol. Life Sci., vol. 59, pp. 959–1023, Jun. 2002.

[8] S. M. Ridha, Z. T. Ghaleb, and A. M. Ghaleb, "The computational investigation of IR and UV-Vis spectra of 2-isopropyl-5-methyl-1,4-benzoquinone using DFT and HF methods," East Eur. J. Phys., vol. 2, no. 1, pp. 197–204, Mar. 2023.

[9] S. M. Ridha, Z. T. Ghaleb, and A. Ghaleb, "Theoretical investigation of the effects of solvents and para-substituents," Rev. Mex. Fis., vol. 71, no. 1 Jan-Feb, pp. 010401-1, Jan. 2025.

[10] C. Møller and M. S. Plesset, "Note on an approximation treatment for many-electron systems," Phys. Rev., vol. 46, p. 618, 1934.

[11] M. J. Frisch et al., Gaussian 09, Revision A.02, Gaussian, Inc., Wallingford, CT, 2009.

[12] R. Ditchfield, W. J. Hehre, and J. A. Pople, "Self-consistent molecular orbital methods. IX. Extended Gaussian-type basis for molecular orbital studies of organic molecules," J. Chem. Phys., vol. 54, pp. 724–730, 1971.

[13] V. Barone and M. Cossi, "Quantum calculation of molecular energies and energy gradients in solution by a conductor solvent model," J. Phys. Chem. A, vol. 102, no. 11, pp. 1995–2001, Mar. 1998.

[14] P. Hohenberg and W. Kohn, "Inhomogeneous electron gas," Phys. Rev., vol. 136, pp. B864–B871, 1964.

[15] R. Bauernschmitt and R. Ahlrichs, "Treatment of electronic excitations within the adiabatic approximation of time-dependent density functional theory," Chem. Phys. Lett., vol. 256, pp. 454–464, 1996.

[16] C. J. Cramer and F. M. Bickelhaupt, "Essentials of computational chemistry," Angew. Chem. Int. Ed. Engl., vol. 42, no. 4, pp. 381–384, 2003.

[17] S. Jafari, M. Cheki, and H. N. Moghadam, "Lomustine and 6 MV X-ray combination effect on U87-MG cancer cells," Pharmacophore, vol. 8, no. 5, pp. 40–46, 2017.

[18] W. Bououden and Y. Benguerba, "Computational quantum chemical study, drug-likeness and in silico cytotoxicity evaluation of some steroidal anti-inflammatory drugs," J. Drug Deliv. Ther., vol. 10, no. 3-s, pp. 68–74, Jun. 2020.